Published in final edited form as:
Biol Bull. 2012 August ; 223(1): 7–20.

Investigating Bacterial-Animal Symbioses with Light Sheet Microscopy

Michael J. Taormina[1,*], **Matthew Jemielita**[1,*], **W. Zac Stephens**[2], **Adam R. Burns**[3], **Joshua V. Troll**[2], **Raghuveer Parthasarathy**[1,2,4,+], and **Karen Guillemin**[2,+]

[1]Department of Physics, University of Oregon, Eugene OR 97403

[2]Institute of Molecular Biology, University of Oregon, Eugene OR 97403

[3]Institute of Ecology and Evolution, University of Oregon, Eugene OR 97403

[4]Materials Science Institute, University of Oregon, Eugene OR 97403

SUMMARY

Microbial colonization of the digestive tract is a crucial event in vertebrate development, required for maturation of host immunity and establishment of normal digestive physiology. Advances in genomic, proteomic, and metabolomic technologies are providing a more detailed picture of the constituents of the intestinal habitat, but these approaches lack the spatial and temporal resolution needed to characterize the assembly and dynamics of microbial communities in this complex environment. We report the use of light sheet microscopy to provide high resolution imaging of bacterial colonization of the zebrafish intestine. The methodology allows us to characterize bacterial population dynamics across the entire organ and the behaviors of individual bacterial and host cells throughout the colonization process. The large four-dimensional datasets generated by these imaging approaches require new strategies for image analysis. When integrated with other "omics" datasets, information about the spatial and temporal dynamics of microbial cells within the vertebrate intestine will provide new mechanistic insights into how microbial communities assemble and function within hosts.

Keywords

light sheet microscopy; microbiota; zebrafish; intestine; in vivo imaging; symbiosis

BACKGROUND AND SIGNIFICANCE

Introduction

All plants and animals are ecosystems for microbial communities. With the advent of high throughput "omics" technologies (including genomics, proteomics, and metabolomics) that can provide comprehensive catalogues of a microbial sample's nucleic acids, proteins, and metabolites, the stature of these underexplored and often overlooked communities is on the rise. Now that we can identify the members of these host-associated microbial communities and their functional capacities, we can ask fundamental questions about these symbiotic associations: How do particular microbial communities assemble on and within hosts? How are these communities maintained over time? How do these communities influence the development and physiology of their hosts? These questions are further motivated by human

[+]corresponding authors: Raghuveer Parthasarathy, raghu@uoregon.edu, Karen Guillemin, guillemin@molbio.uoregon.edu.
[*]co-first authors

health concerns, as recent insights suggest that many diseases, including inflammatory bowel diseases, type II diabetes, colorectal cancer, autoimmune diseases, and possibly even autism, are correlated with altered gut microbiota (Dethlefsen *et al.*, 2007, Spor *et al.*, 2011). A still deeper question in the field of symbiosis is the extent to which there are universal rules and mechanisms that govern the coexistence of plants and animals with their microbial associates and whether lessons learned from model symbioses can be applied to the associations between humans and their complex microbial consortia.

Although they provide extraordinarily powerful tools for probing multi-species systems, "omics" approaches only deliver homogenized inventories of community components, incapable of revealing the spatial organization and dynamics of host-associated microbial communities. To truly understand these associations, we need to be able to visualize them on the spatial and temporal scales at which microbes operate -- an experimental challenge. Here we describe the application of light sheet microscopy to the field of symbiosis. In particular we describe the utility of this imaging technique for exploring unanswered questions about the microbial colonization of the vertebrate intestine using the model organism, zebrafish. Hand in hand with "omics" technologies has come an explosion of data, spurring the need for analytic approaches that can make sense of information being generated about host-associated microbiota. A major thrust of these approaches is to draw correlations between the composition of a microbial community and the physiology of the colonized host (Kuczynski *et al.*, 2012). Analogously, large datasets documenting the three-dimensional spatial distributions of microbial and host cells over time can be analyzed to reveal spatial and temporal correlations between microbial species and between microbes and host cells to build quantitative models of microbial dynamics within a host organ.

One instructive example of insights into host colonization by bacteria comes from live imaging of the partnership between the bobtail squid *Euprymna scolopes* and the luminescent marine bacterium *Vibrio fischerii*, which colonizes the light organ of its host and provides light to erase the squid's shadow when foraging at night in shallow seawater (Nyholm and McFall-Ngai, 2004). Direct visualization of colonization using fluorescently labeled bacteria revealed host-mediated control of the microbial population, as the symbionts are selectively recruited from the seawater and collected on specialized mucus-rich external surfaces before migrating into the pores leading to light organ (Nyholm *et al.*, 2002, Nyholm *et al.*, 2000). The squid maintains long-term control over its symbiont population by purging the contents of the light organ each dawn, thereby allowing a fresh population to regrow from a small residual inoculum (Boettcher *et al.*, 1996). In this simple system, bacterial growth can be well described by analogy to bacterial population dynamics in a flask. An initial clonal inoculum grows exponentially until the population reaches a maximum density and the diurnal venting of the squid is the equivalent of diluting the culture into a flask of fresh broth.

In contrast to the squid light organ, the vertebrate intestine is an open-ended tube with continual flux of microbial and dietary contents. Experimentally, researchers have attempted to model this system as a series of chemostats with climax populations of bacteria maintained at a fixed density by a continual influx of nutrients and efflux of contents (Macfarlane *et al.*, 1998). In reality, we know very little about the microbial population dynamics within this organ and the extent to which the chemostat model accurately recapitulates the intestinal environment. For example, to what extent is the efflux balanced by regrowth of permanent residents, as in a chemostat or the squid light organ, as opposed to influx of new members from the external environment? Are there conditions that favor internal regrowth versus influx? Answers to these questions are crucial for developing treatments for human disease that minimize disturbances of gastrointestinal ecology or that maximize invasion, for example by a probiotic. To investigate colonization of the vertebrate

intestine, one needs an experimentally tractable model vertebrate that can be subject to live imaging. Ideally the host would be optically transparent, small enough to visualize its entire digestive tract, and amenable to microbiological manipulations, such as the ability to generate gnotobiotic animals with defined microbial associations. The zebrafish larva offers all of these features, as well as a rich research history that has generated many valuable protocols and reagents for experimental manipulations.

Zebrafish as a Model for Studying Colonization of the Vertebrate Gut

Zebrafish were pioneered as a model for studying vertebrate development because of their optical transparency, rapid embryonic development, fecundity, inexpensive husbandry, and the ability to manipulate them genetically and embryologically (Grunwald and Eisen, 2002). These same attributes make them extremely useful for studying host-microbe associations (Cheesman and Guillemin, 2007, Kanther and Rawls, 2010). Zebrafish first encounter microbes in their environment at the time when they hatch out of their chorions as larvae between 2 and 3 days post fertilization (dpf). By 4 dpf, their digestive tracts are open to the environment at both ends and begin to be colonized by bacteria in their environment. At 7 dpf, the larval stage shown in Figure 1, they are still optically transparent and their internal organs, including the intestine, can be readily visualized. Their ex-utero development enables easy derivation of germ-free or axenic zebrafish larvae by surface sterilization of the chorion prior to hatching (Milligan-Myhre *et al.*, 2011). Because of their fecundity and the ability to fertilize embryos in vitro, it is possible to derive thousands of germ-free individuals at a time, a scale that is unobtainable in mammalian systems. Our gnotobiotic methodologies have allowed us to infer the roles that the resident microbiota play in host development by comparing the traits of germ-free and conventionally reared zebrafish (Bates *et al.*, 2007, Bates *et al.*, 2006, Cheesman *et al.*, 2011). The ability to rear germ-free zebrafish also provides a starting point for visualizing the process of colonization in real time.

Zebrafish, like all vertebrates, are colonized by complex microbial communities, with the most numerically abundant communities being found in their digestive tracts. Similar to humans, the gut microbiota of zebrafish are dominated by a small number of bacterial phyla, with a high diversity of species and strains within these phyla (Rawls *et al.*, 2006). In teleost fish the dominant phylum is the Proteobacteria (Roeselers *et al.*, 2011), which fortuitously contains the most experimentally tractable bacterial species. We and others have successfully genetically engineered a growing number of zebrafish-derived bacteria to express fluorescent proteins for visualizing their interactions with host tissues and cells. Direct visualization of infection by pathogenic bacteria in zebrafish has upended conventional wisdom about aspects of infectious disease, for example demonstrating the dynamic nature of mycobacterial granulomas (Davis and Ramakrishnan, 2009). The first description of bacterial dynamics in the zebrafish intestine by Rawls and colleagues used widefield fluorescence microscopy (Rawls *et al.*, 2007). These authors described different types of bacterial movement in the intestinal habitat including active swimming and passive movement of large clumps of bacteria. Their studies were limited however by the lack of optical sectioning and three-dimensional resolution inherent in widefield imaging. Below we describe imaging technology that overcomes these limitations.

Four-Dimensional Microscopy and Light Sheet Imaging

Three-dimensional fluorescence imaging of live specimens over time, often denoted four-dimensional microscopy, provides molecule-specific, non-destructive information about the spatial structure and temporal dynamics of biological systems. Four-dimensional imaging of host and microbial cells in a developing intestine presents particular technical challenges, as it simultaneously demands fine spatial resolution to visualize individual cells, fine temporal

resolution to track individual motions and cellular shape changes, large fields of view spanning, for example, a several hundred micron long larval zebrafish intestine, and low levels of photodamage to enable nondestructive imaging over hours or days. There exist a variety of three-dimensional imaging techniques, the most widely adopted of which are confocal and multiphoton microscopies, all of which provide access to different ranges of resolution, speed, photodamage, and tissue penetration. A rather new approach, light sheet fluorescence microscopy, offers a route to high speed, light-efficient imaging of large-scale systems such as developing animals (Keller *et al.*, 2008) and is particularly well suited to visualizing host-associated microbes *in vivo*, as we show here.

The performance characteristics that differentiate light sheet methods and other three-dimensional fluorescence microscopies are straightforward consequences of their geometries. As illustrated in Figure 2A, simple wide-field microscopy is incompatible with optical sectioning of a sample. Light emitted by points in the focal plane of an objective lens is mapped onto points on a detector (typically a camera). Points outside this plane, however, are also excited, emitting light that reaches the detector as an out of focus blur, reducing contrast and destroying depth information. Point scanning confocal microscopy rectifies the problem at the cost of imaging speed and photon efficiency. As shown in Figure 2B, an excitation laser is focused into the specimen, exciting a point in the focal plane as well as points throughout roughly conical volumes around this point. Placement of a pinhole in a conjugate plane blocks most of the light emitted by non-focal points, allowing the in-focus signal to be collected at a detector. At any point in time information is collected from just one point, though a considerably larger volume is illuminated and subject to photodamage. This point must be scanned through all three dimensions to construct a three-dimensional image. Clever use of multiple focal points and pinholes in spinning disk confocal microscopy speeds up this process but retains the intrinsic illumination inefficiency. Multiphoton microscopy (Figure 2C) involves excitation of fluorophores with light of wavelengths two (or more) times that of the normal excitation. The probability of mulitphoton excitation is a nonlinear function of intensity, and hence is appreciable only near the focal point, so it is primarily light from this point that is collected at the detector (Figure 2C). As with confocal microscopy, the focal point of the laser must be scanned to obtain a rasterized optical section or three-dimensional image.

The distinguishing characteristic of light sheet fluorescence microscopy is that it illuminates the entire focal plane from the side, exciting all points in the plane, and capturing all of their emission at once with a camera as in wide-field imaging (Figure 2D). Points outside of the focal plane are not excited and do not contribute to the image. Imaging an entire plane at once provides a dramatic advantage in speed compared to point scanning methods. Moreover, illuminating only the focal plane is intrinsically photon-efficient: there is (ideally) a one-to-one correspondence between illuminated and imaged points, minimizing photobleaching and photodamage by orders of magnitude compared to confocal and multiphoton methods (Keller *et al.*, 2008, Truong *et al.*, 2011). A disadvantage of light sheet microscopy compared to confocal and multiphoton imaging is resolution, a consequence of sheet illumination. Generating a uniform, thin plane of excitation light is made difficult by the diffraction of light; the thinner one makes the center of the sheet, the smaller the lateral extent of this thin region. Issues of axial resolution and field uniformity can be overcome, however, by a variety of adaptations including multi-view reconstruction (Keller *et al.*, 2008, Swoger *et al.*, 2007), structured illumination (Keller *et al.*, 2010, Planchon *et al.*, 2011), non-Gaussian laser beam profiles (Planchon *et al.*, 2011), and two-photon sheet excitation (Truong *et al.*, 2011). In general, light sheet microscopy is amenable to many sorts of modifications and variations. This feature, together with a rather complex history (Santi, 2011), has unfortunately led to a proliferation of names and acronyms – light sheet fluorescence microscopy (LSFM), selective plane illumination microscopy (SPIM), digital

scanned light sheet microscopy (DSLM), orthogonal-plane fluorescence optical sectioning (OPFOS), and more all refer to essentially the same combination of sheet illumination and perpendicular detection. For the purposes of this discussion, we use the term light sheet microscopy to refer to this technology collectively.

MATERIALS AND METHODS

Light Sheet Microscope Design

Light sheet microscopes are to date commercially unavailable, necessitating custom constructions. Various microscope designs and their use in developmental biology have recently been reviewed (Huisken *et al.*, 2004), so we will briefly note the design considerations underlying our home-built light sheet microscope setup (Figure 3), which largely mirrors that of Keller et al. (Keller *et al.*, 2008). A list of key components is provided in Table 1. Multiple laser lines are used to excite different fluorescent probes, e.g. labels of different microbial populations or host cells. Our setup uses single-photon excitation; though multiphoton light sheet excitation can provide enhanced tissue penetration and resolution (Truong *et al.*, 2011), its implementation requires expensive pulsed laser sources and, moreover, may be non-trivial to integrate with multicolor imaging due to the large spectral bandwidth of short laser pulses (Butko *et al.*, 2011). Rapid switching between colors is provided by an acousto-optic tunable filter. The emerging light is incident on a mirror that rapidly scans the beam. A telecentric scan lens transforms the angular scan into a translating scan that when imaged through the tube lens and objective lens produces a sheet of illumination in the specimen. Alternatively, a laser sheet can be formed by focusing a laser beam through a cylindrical lens (Huisken *et al.*, 2004); while this avoids the need for scanning, interference between scattered light from different parts of the sheet can degrade image quality and resolution. Each optical section is imaged through an (orthogonally mounted) high numerical aperture (NA) objective lens and captured by a fast, high resolution camera. Because of its wide-field method of image collection, the limiting factor for imaging speed in light sheet microscopy is the read-out of large resolution sensors; in order to maximize image acquisition speed, we employ a recently developed CMOS camera that has high readout speeds, resolution, sensitivity and dynamic range. For some data sets in this paper (Figure 5H–M) deconvolution methods were applied to improve contrast and resolution, using commercially software noted in Supplemental Information.

Interestingly, the sample chamber necessary to house a submerged specimen and water immersion lens creates a non-trivial design hurdle. Although not discussed in the literature, we have found that many light sheet microscope builders experience difficulty obtaining satisfactory designs, and a number of different configurations have been explored. The challenge lies in the geometry of the design: one needs to control the position and orientation of the specimen as well as the position of the imaging objective. High NA objectives need an immersion medium with a high index of refraction (relative to air), necessitating that the imaging objective protrude into the sample chamber yet maintain a water tight seal. Linear motion in one dimension is necessary to adjust the focus of this objective. The sample being imaged, however, requires linear motion in three spatial dimensions and rotation about one axis for positioning and scanning. In order to provide the specimen with linear motion in three dimensions, it must be anchored to suitable translation stages (stages that enable linear motion). Because such devices are typically large and non-submersible, control of the specimen is best achieved from above the surface of the liquid medium, leaving access for the imaging objective restricted to one of the vertical walls or the bottom of the chamber.

The illumination objective, in contrast, is typically of low numerical aperture in order to create a small angle of divergence for the sheet, and has a large working distance. It can therefore be kept outside the sample chamber.

The approach to sample chamber design that we have taken is to replace one side with a sheet of silicone rubber that has been custom formed to create a water-tight seal around the imaging objective (Figure 3B). This was accomplished using a commercially available tin-cured silicone molded around a slightly undersized disk to match the objective. Live fish are drawn into a small capillary with low concentration agarose gel. After the gel sets, it is partially extruded out of the capillary such that the specimen is suspended below the end of the glass, with the opposite end attached to the motion control hardware above the specimen chamber.

Regardless of the details of particular designs, light sheet microscopes possess an intrinsic speed and photon efficiency that are useful for large-scale imaging of organisms, as has been demonstrated, for example, by several recent studies (e.g. (Keller *et al.*, 2008, Scherz *et al.*, 2008, Truong *et al.*, 2011)). These characteristics make light sheet methods valuable for studying the dynamics of bacterial-host interactions. The studies illustrated below exemplify the importance of imaging speed, e.g. to discern the motility of individual bacteria, and large fields of view and low levels of photodamage, e.g. to image an entire organ for long times.

Zebrafish Husbandry and Bacterial Colonization

All experiments with zebrafish were performed using protocols approved by the University of Oregon Institutional Animal Care and Use Committee and following standard protocols (Westerfield, 2000). The zebrafish line *Tg[BACmpo:gfp]* (Renshaw *et al.*, 2006) (referred to as *mpo:gfp* below) was used to visualize neutrophils and *Tg[nkx2.2a:mEGFP]* (Ng *et al.*, 2005) (referred to as *nkx2.2a:egfp* below) was used to visualize enteroendocrine cells. Larvae were reared at a density of approximately 1 fish/ml of embryo medium (EM) at 28.5 C. Larvae were not fed during the course of these experiments, instead subsisting off their egg yolks for nourishment. Embryos from natural or *in vitro* fertilization derived crosses of wild-type AB/Tu fish were derived germ-free as described (Milligan-Myhre *et al.*, 2011). Germ-free larvae were inoculated with bacteria at 3 dpf, unless otherwise noted. Larvae were removed from flasks with bacteria, rinsed once in sterile EM and anesthetized in MS222 (tricaine methanesulfonate), then mounted in agar prior to imaging on the light sheet microscope. Anesthetized fish could be maintained for up to 24 hours of continuous imaging. Viability of the fish was assessed by the beating of the heart and the occurrence of peristalsis in the intestine. We observed, as has been previously noted (Rombough, 2007), that older larval fish were more susceptible to MS222 toxicity, so we employed doses no higher than 80 mg/L and larvae no older than 6 dpf.

Aeromonas veronii strains used to inoculate germ-free fish were grown overnight (16 hours) aerobically at 30 C in Luria broth shaking at 185 RPM prior to inoculation at a target total density of 10^4 CFU/mL in EM. Antibiotics were added to overnight cultures as needed (Kanamycin 100 μg/ml, Gentamycin 10 μg/ml, Rifampicin 100 μg/ml). Strains used were derived from *A. veronii* HM21 (Graf, 1999). The dTomato expressing strain (HMTn7RFP) is derived from a naturally isolated rifampicin resistant strain, HM21R, into which Gm:tac-dTomato (Singer *et al.*, 2010) was inserted by Tn7-mediated transposition. The GFP expressing strain (HMTn7GFP) is derived from HM21 into which Kan:GFP was inserted by Tn7-mediated transposition. The doubling times during logarithmic growth at 30 C in Luria broth of the RFP and GFP expressing strains were determined to be 38.8 minutes and 39.1 minutes respectively.

RESULTS

Visualizing Bacterial Colonization Dynamics in the Zebrafish Intestine

To begin to investigate bacterial colonization dynamics in the zebrafish intestine using light sheet microscopy, we performed experiments in which we inoculated initially germ-free larvae with fluorescently labeled *Aeromonas veronii*, a common bacterial resident of the zebrafish intestine, and imaged over an extended time period. We incubated the fish with the bacteria for 6 hours prior to imaging, which was the shortest inoculation time that ensured consistent colonization across all of the fish. *A. veronii* colonization of the germ-free intestine could occur by many possible mechanisms. In one extreme model, a single bacterial cell could colonize the organ and clonally expand. A second model, at the opposite extreme, would involve continuous influx and efflux of bacterial cells, with no growth occurring within the intestine itself. A third model, commonly evoked in the human gastrointestinal literature, posits that microbial growth in the intestine resembles growth in a chemostat (Macfarlane *et al.*, 1998), with bacterial cell proliferation being driven by influx of nutrients into the system and balanced by efflux of contents out of the system. To discriminate between these and other possible colonization dynamic models, we simultaneously exposed germ-free zebrafish larvae to two isogenic strains of wild type *A. veronii* with similar in vitro growth rates, one expressing green fluorescent protein (HMTn7GFP) and the other dTomato (HMTn7RFP). The larvae were incubated with the bacterial strains for six hours, after which three-dimensional images spanning the entire intestine were collected every 20 minutes for 18 hours. Each three-dimensional data set, roughly 3 GB in size, was obtained in approximately 60 seconds per color channel.

In all fish examined, we observed both fluorescently marked *A. veronii* strains within the zebrafish intestine (Figure 4), ruling out the first model of colonization by a single cell. The second model of continuous influx of bacteria from the environment without population growth in the intestine was also not supported by our data. In media in which the fish were inoculated, we observed a well-mixed distribution of red and green cells in suspension and some clumps of cells that contained both red and green members (Figure 4A). The pattern of multicolored clumps of cells is expected because the cells are genetically identical except for the fluorescent proteins they produce and thus should have no bias for homotypic aggregation. In contrast, in the fish intestines we observed single-colored aggregates of cells, which we interpret to occur through clonal expansion of single cells (Figure 4B–J and Supplemental Figure 1). We speculate that some of the larger clumps consist of clonally expanded cells adhering in biofilms to flocculent material such as host mucus or dead cells shed from the intestinal epithelium (Sonnenburg *et al.*, 2004). Interestingly, some of these clumps persist for long periods of time, others transit through the intestine rapidly, while still others disintegrate or become dislodged from formerly stable locations, indicating that the fluid dynamics within this organ are extremely complex. The heterogeneous distribution of clumps of bacterial cells we observed was also inconsistent with the model of a well-mixed chemostat, although more complex models of unmixed chemostats could apply (Smith and Waltman, 1995).

The light sheet microscope allows us to monitor bacterial population abundance and dynamics in real time in the zebrafish intestine. Some of the fluorescent signal observed emanated from the fish tissue itself, as is apparent when we image germ-free animals or animals colonized with low numbers of bacteria. Certain host cells of unknown identity emit very bright autofluorescent signals, but these are easily distinguished from colonizing bacteria because of their large size, their position outside of the gut lumen, and the fact their autofluorescence is detected in both the red and green channels. The intensities of red and green fluorescence within the intestinal lumen, when threshholded to remove low level fluorescent background, correlates fairly well with the relative abundance of red and green

labeled cells, as measured by dilution plating (Supplemental Figure 2), validating our use of fluorescence intensity as a surrogate for bacterial population size and location. In contrast to a chemostat in which the entire volume is occupied by microbial cells utilizing available resources to support their growth, our imaging of the zebrafish intestine revealed bacterial colonization to be spatially highly heterogeneous, with punctate colonies and non-uniform distribution of colonies along the length of the gut (Figure 4B–J and Supplemental Figure 1). Additionally, the spatial distribution of bacteria was highly dynamic, with large changes in overall abundance as well as localization occurring during the imaging period (Figure 4C–J and Supplemental Figure 1). Our observations support two possible models of the intestinal environment, which are not mutually exclusive: first that resources for bacterial growth are distributed non-uniformly and highly dynamically in the zebrafish intestine, and second that other determinants, such as peristaltic forces or immune cell surveillance, play significant roles in bacterial population distributions. It is clear that the simple model of a chemostat with evenly distributed bacterial cells does not accurately describe the real behavior of bacterial populations in the zebrafish intestine.

The high speed of light sheet fluorescence imaging also enables observations of the motility of individual bacterial cells. Supplemental Movie S1 shows a two-dimensional section of a larval zebrafish intestine with dTomato–labeled *A. veronii* bacteria (HMTn7RFP) (as in Figure 4). Several distinct motility patterns are evident, including stationary clumps of bacteria, bacteria passively moving with the fluid flow, and actively swimming bacteria. While motility is relatively straightforward to study *in vitro*, its properties *in vivo* are largely unexplored and may not reflect those of cultured bacteria due both to the complex physical environment of the intestine and to signaling among intestinal constituents. Future analyses of bacterial cell dynamics in the zebrafish intestine will investigate how individual cells explore their local chemical and spatial environments and address questions about the proportion of the community that are permanent residents as opposed to transients and whether motility is a prerequisite for permanent residency. *Aeromonas* species are of particular interest, as they have been shown to chemotax towards fish mucus (van der Marel *et al.*, 2008) and exhibit different modes of motility mediated by different types of flagella (Altarriba *et al.*, 2003).

Visualizing Host Cell Dynamics in the Intestine

An important question in the field of symbiosis is how the process of colonization and the presence of microbial associates change the development and function of the host. We have characterized numerous zebrafish traits that are affected by the microbiota. For example, germ-free zebrafish intestines have a paucity of secretory cells, including hormone-secreting enetroendocrine cells, and neutrophils, phagocytic cells of the innate immune system (Bates *et al.*, 2007, Bates *et al.*, 2006). In addition, the physiology of the intestine is altered in the absence of the microbiota, with more rapid peristaltic contractions (Bates *et al.*, 2006). The high speed of light sheet microscopy provides an opportunity to explore host-microbe interactions at much higher resolution and to ask how the microbiota affect the dynamics of individual zebrafish cells, and reciprocally, how host cells affect the microbiota.

To demonstrate the feasibility of this approach, we used the transgenic zebrafish line *nkx2.2a:egfp*, which drives expression of a membrane bound GFP in enteroendocrine cells in the intestinal epithelium (Ng *et al.*, 2005). Six dpf larvae were imaged for several hours (Figure 5A–G and Supplemental Movie S2), demonstrating the ability of future in-depth studies to follow the genesis of these cells in the presence and absence of microbiota. Imaging also shows the dynamics of these cells and emphasizes the extent to which they experience mechanical forces during the propulsion of peristaltic waves along the length of the intestine; cell shape distortions are clearly visible during such a contraction (Figure 5A–

F and Supplemental Movie S2). Typical image acquisition timescales, roughly tens of ms for two-dimensional slices and a few seconds for three-dimensional images, are faster than the periodicity of peristalsis, allowing imaging without motion-induced blurring. Since there are fewer of these cells in the germ-free intestine, and since these cells produce hormones that regulate peristalsis, we expect to observe interesting changes in the cellular and organ-wide contractile behaviors during colonization.

In addition to the cells of the intestinal epithelial, gut microbes interact with immune cells that actively survey this tissue. Neutrophils are important first responders to intestinal infections and we have shown that these cells are also recruited to the intestine upon colonization by the microbiota (Bates *et al.*, 2007). Being highly motile and responsive to chemical cues, neutrophils are a model cell for chemotaxis studies, and their *in vivo* behavior has been characterized extensively in zebrafish using confocal microscopy (e.g. (Colucci-Guyon *et al.*, 2011, Feng *et al.*, 2010, Yoo *et al.*, 2010)). Visualizing their dynamics in internal tissues such as the intestine, however, poses technical challenges that we were able to overcome using light sheet microscopy. We visualized GFP labeled neutrophils in the *mpo:gfp* transgenic line (Renshaw *et al.*, 2006) at various ages from 4–8 dpf in time lapse z-scans of the whole intestine for several hours. We obtained scans spanning 60 μm thick intestines with optical slices separated by 1 μm in as little as 12 s per three-dimensional data set. The speed and range of imaging allowed us to identify neutrophils undergoing active processes at different depths throughout the intestine, and we were able to visualize individual cell shape rearrangements such as the extension and retraction of filopodia (Figure 5H–M). Simultaneously imaging fluorescently labeled bacteria and neutrophils with light sheet microscopy will enable visualization of neutrophil recruitment to the intestine upon bacterial colonization and will address whether they exhibit different behaviors, such as increased filopodia activity, in the presence of commensal microbes. We will also be able to explore the possibility that neutrophils influence bacterial population growth dynamics by examining correlations between local heterogeneities in the microbiota and the positions of neutrophils.

Analyzing *in vivo* Cell Population Dynamics

Live imaging of intestinal bacteria with high spatial and temporal resolution over hours or days produces a vast quantity of image data. The two-color imaging of gut microbes illustrated in Figure 4, for example, yielded over 300 GB of images from a single larval zebrafish; this number could be easily increased with finer temporal sampling or a greater number of labeled populations. Like other recently developed biological techniques, such as high-throughput sequencing and proteomic methods, light sheet imaging shares the challenge of extracting comprehensible insights from high volumes of data. It is likely that a variety of approaches to this task will be developed as data sets become available. We suggest here a few promising perspectives.

The raw data output by light sheet imaging of fluorescently-labeled intestinal microbes denote the density of bacteria over time and three-dimensional space. A simple distillation of this information is provided by collapsing this density onto the axis provided by the gut itself, integrating the intensity of image slices perpendicular to the gut center-line at each point along the line, yielding a one-dimensional measure of bacterial population along the anterior-posterior coordinate. This one-dimensional projection can be performed for each measurement time, as illustrated in Figure 6 for the data set from which Figure 4 was extracted. From this and other observations, it is evident that bacterial populations are not homogeneously distributed along the gut. One can correlate the existence of preferential locations for bacterial growth with anatomical position, noting for example high population density in the most anterior and posterior regions of the intestine. Moreover, it is evident that

the dynamics of growth are complex; the spatially non-uniform distribution present initially is not simply scaled or magnified as time progresses, but rather varies non-monotonically over the course of hours.

While projections are easily comprehensible, they necessarily neglect three-dimensional structure and dynamics. Considering interacting bacterial species, it will likely be fruitful to investigate spatial correlation functions that involve different microbial groups. Co-localization, anti-localization, and spatially offset population densities can reveal the functional relationships between species that cooperate, compete, or interact via exchange of metabolites. Correlation functions moreover can provide a measure of structure that maps higher-dimensional organization onto visualizable lower-dimensional spaces.

To illustrate this, we first consider the schematic, computer-generated image in Figure 7A, in which green spots are distributed randomly in two dimensions, and slightly larger red spots are positioned such that each is some particular distance (here, 20 ± 1 pixels) from a green spot, in a random direction. By construction, the correlation between red and green is not perfectly sharp. For each green spot, there is a red spot placed 20 +/− 1 px away. This red spot may be less than or greater than 20 px distant from other green spots. This correlation between the red and green structures in Figure 7A is not apparent by eye. Denoting the intensity of pixels in the green and red channels I_g and I_r, respectively, the normalized cross-correlation is given by (Gonzalez and Woods, 1992)

$$C_{gr}(\vec{\rho}) = \frac{\sum \left(I_g(\vec{r}) - \langle I_g \rangle\right)\left(I_r(\vec{r} - \vec{\rho}) - \langle I_r \rangle\right)}{\left[\sum \left(I_g(\vec{r}) - \langle I_g \rangle\right)^2 \sum \left(I_r(\vec{r} - \vec{\rho}) - \langle I_r \rangle\right)^2\right]^{0.5}}.$$

where $r\rightarrow$ indicates position, $\rho\rightarrow$ is the spatial offset, the angle brackets indicate the average intensity, and the sums run over all pixels in an image. If the two intensity distributions are spatially offset by some well-defined amount, the numerator in the above expression will be large when $\rho\rightarrow$ equals that amount, and C_{gr} will have a peak at that offset. This is evident in Figure 7B, which shows C_{gr} ($\rho\rightarrow$) for the image in Figure 7A, yielding a ring at a displacement of 20 pixels from the origin. In Figure 7C we show C_{gr} (ρ), the correlation as a function of radial displacement $\rho = |\rho\rightarrow|$, i.e. averaged over angle. Again, a 20 pixel offset is apparent.

Particular coordinate systems can help characterize particular spatial distributions of bacterial populations. For example, by determining the gut center line (either manually or by computational analysis of the bounded space), one can define a cylinder-like coordinate system, the radial component of which distinguishes luminal and mucosal positions in the gut. Considering cross-correlations in which $\rho\rightarrow$ is the radial coordinate, situations in which one population is predominantly mucosal and the other is predominantly luminal would give a peak in C_{gr} at some radial displacement.

The auto-correlation of each intensity function (i.e. its correlation with itself) also provides useful information. C_{gg} ($\rho\rightarrow$) and C_{rr} ($\rho\rightarrow$) each trivially have a peak at $\rho\rightarrow = 0$, as any function is perfectly correlated with itself; these autocorrelations decay with a characteristic scale equal to the typical object size in the intensity images. We see this decay in Figure 7C; as expected, the red autocorrelation curve has a larger decay length, as it corresponds to the larger particle size.

In contrast, Figures 7D–F show simulated images and the resulting calculated correlations for images in which the position of both the red and green spots were completely random. For such distributions, the cross-correlation has a low, featureless value.

We provide an example of correlation function analysis of real three-dimensional bacterial images in Figure 7G,H. The source data are from the same setup as illustrated in Figure 4: two-color images of *A. veronii* HMTn7GFP and HMTn7RFP in the intestine. The intensity correlations shown in Figure 7H are calculated from a 166×333×64 μm^3 volume at a single time point, one optical section of which is depicted in Figure 7G. The autocorrelations are similar in each color channel with a characteristic length-scale of a few μm. The cross-correlation is small and featureless, as expected, as these two populations are biologically identical and should be randomly situated.

More generally, we can expect different sorts of correlations from more complex sets of species, and a key goal of this article is to encourage progress along these lines. A lack of cross-correlation near $\rho\rightarrow = 0$, for example, can indicate competing species that are unlikely to occupy the same spatial niche. Strong correlation at some non-zero distance can reveal, for example, cooperating species whose interactions are mediated by the exchange of metabolic products whose dispersal spans some characteristic range. Of course, using cross-correlations to compare groups requires assessment of the precision of multi-color image registry, which can be compromised by both optical aberrations and by motions of the specimen. Control images can be provided, for example, by larvae that have ingested multi-color fluorescent beads, the images from which should be perfectly correlated. The use of autocorrelations to determine typical colony sizes requires no such multi-color registry, and in itself can reveal features of importance such as the growth of typical colony sizes with time.

It should also be possible to use characterizations of bacterial motility, enabled by the high speed of light sheet microscopy as noted above, to examine spatial correlations between differently motile groups. Using either temporal correlations between images or direct tracking of moving microbes, bacterial populations with the same fluorescent reporters can be divided into categories of different motilities, and spatial correlations between these sub-populations could be examined using the same approach described above. We expect that such studies may illuminate connections between microbial behaviors and gut colonization.

DISCUSSION

Advances in genomics, proteomics, and metabolomics have generated an explosion of information about the bacterial associates of humans (Kuczynski *et al.*, 2012). This flood of data is enabling new approaches to modeling the metabolic activities and ecological interactions of host-associated microbial communities (e.g. (Borenstein *et al.*, 2008, Greenblum *et al.*, 2012)), which will enrich the entire field of symbiosis. These approaches, however, are based on samples that are homogenized mixtures of microbes at a single point in time, and they fail to take into account the complex spatial dynamics of microbial populations (Green *et al.*, 2008).

The study of spatial population dynamics has a long history in ecology (Huffaker, 1958). The application of these ideas to naturally occurring microbial communities, however, has been hindered by the technical challenges of observing population dynamics on the spatial and temporal scales of microbes. Here we present the methodology of light sheet microscopy and its application to visualizing the dynamics of zebrafish intestinal microbiota and associated host cells. The spatial resolution and non-destructive sampling of light sheet imaging will provide researchers with new opportunities to apply ecological theories and concepts to the study of host-associated microbial communities.

Four-dimensional imaging will afford the opportunity to study the colonization and succession of gut microbial communities (Fierer *et al.*, 2010), determining where in the

intestine microorganisms first establish and how this influences the ability of successive colonizers to invade. The mechanisms that drive and control the population dynamics of bacterial species, (e.g. dispersal, trophic interactions, environmental pressures), can be inferred by examining patterns of the synchrony of populations across space and time (Bjornstad *et al.*, 1999). Further questions that can be illuminated with this technology include whether succession is driven more by expansion from initial colonizers or from continued migration, how communities respond to disturbances (secondary succession), and where these dynamics occur with relation to host cells and landmarks. Light sheet imaging is particularly useful for visualizing the dynamics of symbiosis in live animals because of the speed of image acquisition and low photodamage. Light sheet imaging could be employed to image microbial colonization of the internal organs of transparent animals, including many marine organisms and insect larvae, and to record bacterial associations of surface tissues of any animal or plant. We speculate that it will be especially powerful when applied to model symbiosis systems of bacterial associations with the squid light organ, the leech crop, the fruit fly and nematode digestive tracts, and fungal and bacterial interactions with plant roots and rodent skin.

Here we have presented results that demonstrate the feasibility of using light sheet imaging to characterize the bacterial colonization of the zebrafish intestine and the host's response to this colonization at a resolution that informs us about the behaviors of individual cells and the dynamics of entire populations of cells. We discuss the challenges of making sense of the vast amounts of image data generated by this four-dimensional microscopy and present approaches to analyzing and interpreting correlations between different simultaneously imaged cell populations. An important future goal will be to integrate other types of "omics" data with *in vivo* imaging of host-associated microbial communities. Although this will be a formidable challenge, we believe that taking into account spatial organization and temporal dynamics of complex microbial communities resident on animals will be essential for understanding these communities' metabolic activities and the causes and consequences of those activities. In comparison to all other bacterial communities sampled across the globe, the communities found within the vertebrate intestine have a unique and unusual phylogenetic composition (Ley *et al.*, 2008). We suspect that vertebrate intestinal microbiota will also posses unique spatial organizations and temporal dynamics that can not be approximated by models such as the chemostat, which fails to take into account the complex reciprocal interactions between the microbes and their host environment. Direct visualization of these microbe-host interactions is the first important step towards understanding the growth, development, and function of these microbial communities that are integral to animal biology.

Supplementary Material

Refer to Web version on PubMed Central for supplementary material.

Acknowledgments

We thank Jennifer Hampton for contributions to this work, Richard Suhr and Richard Holton for experimental assistance, and Brendan Bohannan for insightful discussions. This work was funded by NSF grant 0922951 to R.P. and NIH grant 1R01GM095385 to K.G; M.T. was supported on NSF GK12 grant 0742540; W.Z.S was supported on NSF IGERT grant DGE 9972830; and J.V.T. was supported on NIH NRSA 1F32DK089716 and American Cancer Society Fellowship 120188-PF-11-272-01-MPC. NIH grant HD22486 provided support for the Oregon Zebrafish Facility.

Abbreviations

dpf	days post fertilization
EM	embryo medium
GFP	green fluorescent protein
NA	numerical aperture

REFERENCES

Altarriba M, Merino S, Gavin R, Canals R, Rabaan A, Shaw JG, Tomas JM. A polar flagella operon (flg) of Aeromonas hydrophila contains genes required for lateral flagella expression. Microb Pathog. 2003; 34:249–259. [PubMed: 12732473]

Bates JM, Akerlund J, Mittge E, Guillemin K. Intestinal alkaline phosphatase detoxifies lipopolysaccharide and prevents inflammation in zebrafish in response to the gut microbiota. Cell Host Microbe. 2007; 2:371–382. [PubMed: 18078689]

Bates JM, Mittge E, Kuhlman J, Baden KN, Cheesman SE, Guillemin K. Distinct signals from the microbiota promote different aspects of zebrafish gut differentiation. Dev Biol. 2006; 297:374–386. [PubMed: 16781702]

Bjornstad ON, Ims RA, Lambin X. Spatial population dynamics: analyzing patterns and processes of population synchrony. Trends Ecol Evol. 1999; 14:427–432. [PubMed: 10511718]

Boettcher KJ, Ruby EG, McFall-Ngai MJ. Bioluminescence in the symbiotic squid Euprymna scolopes is controlled by a daily biological rhythm. Journal of Comparative Physiology A Sensory Neural and Behavioral Physiology. 1996; 179:65–73.

Borenstein E, Kupiec M, Feldman MW, Ruppin E. Large-scale reconstruction and phylogenetic analysis of metabolic environments. Proc Natl Acad Sci U S A. 2008; 105:14482–14487. [PubMed: 18787117]

Butko MT, Drobizhev M, Makarov NS, Rebane A, Brinkman BC, Gleeson JG. Simultaneous multiple-excitation multiphoton microscopy yields increased imaging sensitivity and specificity. BMC Biotechnol. 2011; 11:20. [PubMed: 21366923]

Cheesman SE, Guillemin K. We know you are in there: conversing with the indigenous gut microbiota. Res Microbiol. 2007; 158:2–9. [PubMed: 17223317]

Cheesman SE, Neal JT, Mittge E, Seredick BM, Guillemin K. Epithelial cell proliferation in the developing zebrafish intestine is regulated by the Wnt pathway and microbial signaling via Myd88. Proc Natl Acad Sci U S A. 2011; 108(Suppl 1):4570–4577. [PubMed: 20921418]

Colucci-Guyon E, Tinevez JY, Renshaw SA, Herbomel P. Strategies of professional phagocytes in vivo: unlike macrophages, neutrophils engulf only surface-associated microbes. J Cell Sci. 2011; 124:3053–3059. [PubMed: 21868367]

Davis JM, Ramakrishnan L. The role of the granuloma in expansion and dissemination of early tuberculous infection. Cell. 2009; 136:37–49. [PubMed: 19135887]

Dethlefsen L, McFall-Ngai M, Relman DA. An ecological and evolutionary perspective on human-microbe mutualism and disease. Nature. 2007; 449:811–818. [PubMed: 17943117]

Feng Y, Santoriello C, Mione M, Hurlstone A, Martin P. Live imaging of innate immune cell sensing of transformed cells in zebrafish larvae: parallels between tumor initiation and wound inflammation. PLoS Biol. 2010; 8:e1000562. [PubMed: 21179501]

Fierer N, Nemergut D, Knight R, Craine JM. Changes through time: integrating microorganisms into the study of succession. Res Microbiol. 2010; 161:635–642. [PubMed: 20599610]

Gonzalez, RC.; Woods, RE. Digital image processing. Reading, Mass: Addison-Wesley; 1992.

Graf J. Symbiosis of Aeromonas veronii biovar sobria and Hirudo medicinalis, the medicinal leech: a novel model for digestive tract associations. Infect Immun. 1999; 67:1–7. [PubMed: 9864188]

Green JL, Bohannan BJ, Whitaker RJ. Microbial biogeography: from taxonomy to traits. Science. 2008; 320:1039–1043. [PubMed: 18497288]

Greenblum S, Turnbaugh PJ, Borenstein E. Metagenomic systems biology of the human gut microbiome reveals topological shifts associated with obesity and inflammatory bowel disease. Proc Natl Acad Sci U S A. 2012; 109:594–599. [PubMed: 22184244]

Grunwald DJ, Eisen JS. Headwaters of the zebrafish -- emergence of a new model vertebrate. Nat Rev Genet. 2002; 3:717–724. [PubMed: 12209146]

Huffaker C. Experimental Studies of Predation: Disperion Factors and Predator-Prey Oscillations. Hilgardia. 1958; 21:795–835.

Huisken J, Swoger J, Del Bene F, Wittbrodt J, Stelzer EH. Optical sectioning deep inside live embryos by selective plane illumination microscopy. Science. 2004; 305:1007–1009. [PubMed: 15310904]

Kanther M, Rawls JF. Host-microbe interactions in the developing zebrafish. Curr Opin Immunol. 2010; 22:10–19. [PubMed: 20153622]

Keller PJ, Schmidt AD, Santella A, Khairy K, Bao Z, Wittbrodt J, Stelzer EH. Fast, high-contrast imaging of animal development with scanned light sheet-based structured-illumination microscopy. Nat Methods. 2010; 7:637–642. [PubMed: 20601950]

Keller PJ, Schmidt AD, Wittbrodt J, Stelzer EH. Reconstruction of zebrafish early embryonic development by scanned light sheet microscopy. Science. 2008; 322:1065–1069. [PubMed: 18845710]

Kuczynski J, Lauber CL, Walters WA, Parfrey LW, Clemente JC, Gevers D, Knight R. Experimental and analytical tools for studying the human microbiome. Nat Rev Genet. 2012; 13:47–58. [PubMed: 22179717]

Ley RE, Lozupone CA, Hamady M, Knight R, Gordon JI. Worlds within worlds: evolution of the vertebrate gut microbiota. Nat Rev Microbiol. 2008; 6:776–788. [PubMed: 18794915]

Macfarlane GT, Macfarlane S, Gibson GR. Validation of a Three-Stage Compound Continuous Culture System for Investigating the Effect of Retention Time on the Ecology and Metabolism of Bacteria in the Human Colon. Microb Ecol. 1998; 35:180–187. [PubMed: 9541554]

Milligan-Myhre K, Charette JR, Phennicie RT, Stephens WZ, Rawls JF, Guillemin K, Kim CH. Study of host-microbe interactions in zebrafish. Methods Cell Biol. 2011; 105:87–116. [PubMed: 21951527]

Ng AN, de Jong-Curtain TA, Mawdsley DJ, White SJ, Shin J, Appel B, Dong PD, Stainier DY, Heath JK. Formation of the digestive system in zebrafish: III. Intestinal epithelium morphogenesis. Dev Biol. 2005; 286:114–135. [PubMed: 16125164]

Nyholm SV, Deplancke B, Gaskins HR, Apicella MA, McFall-Ngai MJ. Roles of Vibrio fischeri and nonsymbiotic bacteria in the dynamics of mucus secretion during symbiont colonization of the Euprymna scolopes light organ. Appl Environ Microbiol. 2002; 68:5113–5122. [PubMed: 12324362]

Nyholm SV, McFall-Ngai MJ. The winnowing: establishing the squid-vibrio symbiosis. Nat Rev Microbiol. 2004; 2:632–642. [PubMed: 15263898]

Nyholm SV, Stabb EV, Ruby EG, McFall-Ngai MJ. Establishment of an animal-bacterial association: recruiting symbiotic vibrios from the environment. Proc Natl Acad Sci U S A. 2000; 97:10231–10235. [PubMed: 10963683]

Planchon TA, Gao L, Milkie DE, Davidson MW, Galbraith JA, Galbraith CG, Betzig E. Rapid three-dimensional isotropic imaging of living cells using Bessel beam plane illumination. Nat Methods. 2011; 8:417–423. [PubMed: 21378978]

Rawls JF, Mahowald MA, Goodman AL, Trent CM, Gordon JI. In vivo imaging and genetic analysis link bacterial motility and symbiosis in the zebrafish gut. Proc Natl Acad Sci U S A. 2007; 104:7622–7627. [PubMed: 17456593]

Rawls JF, Mahowald MA, Ley RE, Gordon JI. Reciprocal gut microbiota transplants from zebrafish and mice to germ-free recipients reveal host habitat selection. Cell. 2006; 127:423–433. [PubMed: 17055441]

Renshaw SA, Loynes CA, Trushell DM, Elworthy S, Ingham PW, Whyte MK. A transgenic zebrafish model of neutrophilic inflammation. Blood. 2006; 108:3976–3978. [PubMed: 16926288]

Roeselers G, Mittge EK, Stephens WZ, Parichy DM, Cavanaugh CM, Guillemin K, Rawls JF. Evidence for a core gut microbiota in the zebrafish. ISME J. 2011; 5:1595–1608. [PubMed: 21472014]

Rombough PJ. Ontogenetic changes in the toxicity and efficacy of the anaesthetic MS222 (tricaine methanesulfonate) in zebrafish (Danio rerio) larvae. Comp Biochem Physiol A Mol Integr Physiol. 2007; 148:463–469. [PubMed: 17643329]

Santi PA. Light sheet fluorescence microscopy: a review. J Histochem Cytochem. 2011; 59:129–138. [PubMed: 21339178]

Scherz PJ, Huisken J, Sahai-Hernandez P, Stainier DY. High-speed imaging of developing heart valves reveals interplay of morphogenesis and function. Development. 2008; 135:1179–1187. [PubMed: 18272595]

Singer JT, Phennicie RT, Sullivan MJ, Porter LA, Shaffer VJ, Kim CH. Broad-host-range plasmids for red fluorescent protein labeling of gram-negative bacteria for use in the zebrafish model system. Appl Environ Microbiol. 2010; 76:3467–3474. [PubMed: 20363780]

Smith, HL.; Waltman, P. The theory of the chemostat: dynamics of microbial competition. Cambridge: Cambridge university press; 1995.

Sonnenburg JL, Angenent LT, Gordon JI. Getting a grip on things: how do communities of bacterial symbionts become established in our intestine? Nat Immunol. 2004; 5:569–573. [PubMed: 15164016]

Spor A, Koren O, Ley R. Unravelling the effects of the environment and host genotype on the gut microbiome. Nat Rev Microbiol. 2011; 9:279–290. [PubMed: 21407244]

Swoger J, Verveer P, Greger K, Huisken J, Stelzer EH. Multi-view image fusion improves resolution in three-dimensional microscopy. Opt Express. 2007; 15:8029–8042. [PubMed: 19547131]

Truong TV, Supatto W, Koos DS, Choi JM, Fraser SE. Deep and fast live imaging with two-photon scanned light-sheet microscopy. Nat Methods. 2011; 8:757–760. [PubMed: 21765409]

van der Marel M, Schroers V, Neuhaus H, Steinhagen D. Chemotaxis towards, adhesion to, and growth in carp gut mucus of two Aeromonas hydrophila strains with different pathogenicity for common carp, Cyprinus carpio L. J Fish Dis. 2008; 31:321–330. [PubMed: 18355183]

Westerfield, M. The zebrafish book. A guide for the laboratory use of zebrafish (Danio rerio). Eugene: Univ. of Oregon Press; 2000.

Yoo SK, Deng Q, Cavnar PJ, Wu YI, Hahn KM, Huttenlocher A. Differential regulation of protrusion and polarity by PI3K during neutrophil motility in live zebrafish. Dev Cell. 2010; 18:226–236. [PubMed: 20159593]

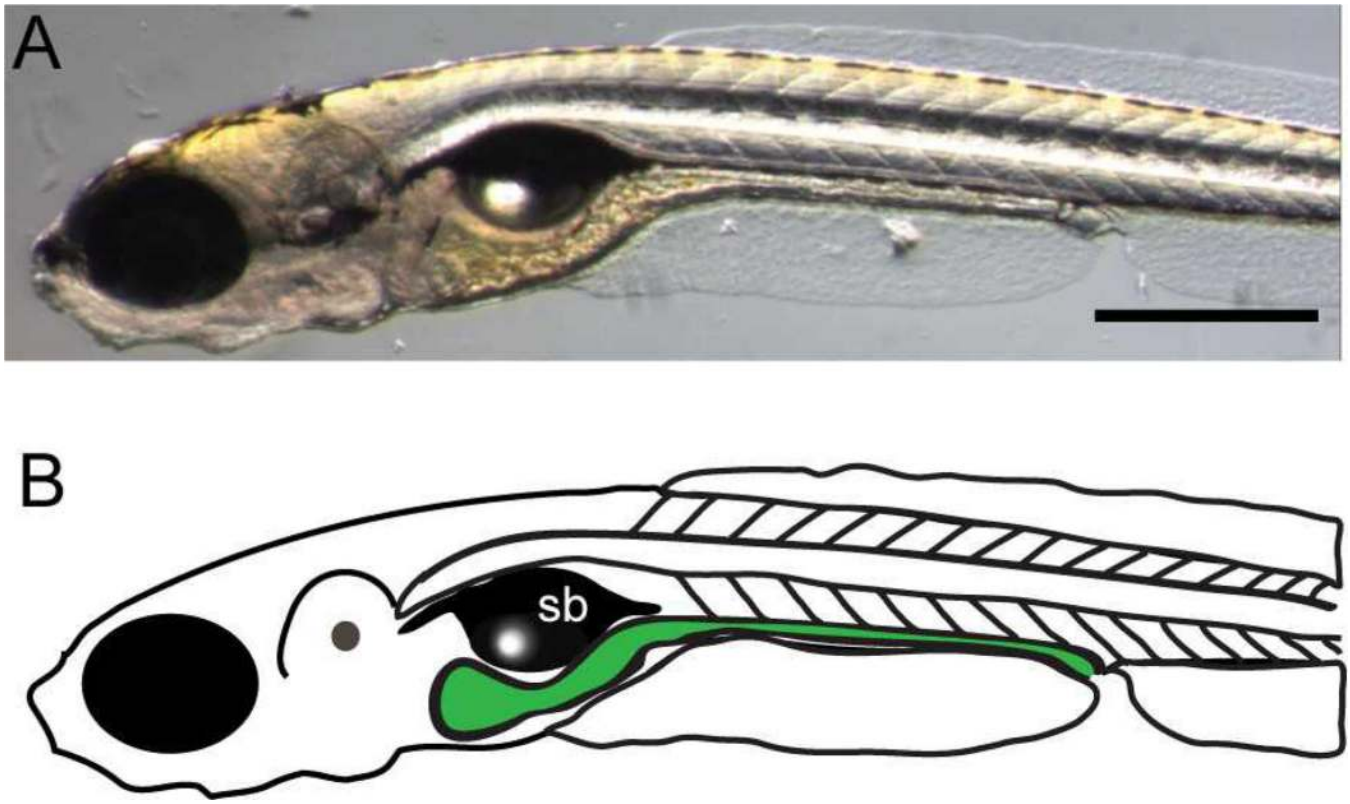

Figure 1.
A 7 dpf zebrafish larva. A brightfield image (A) and a schematic representation (B) illustrating the intestinal tract. sb indicates the swim bladder and grey fill highlights the intestine. Scale bar: 0.5 mm.

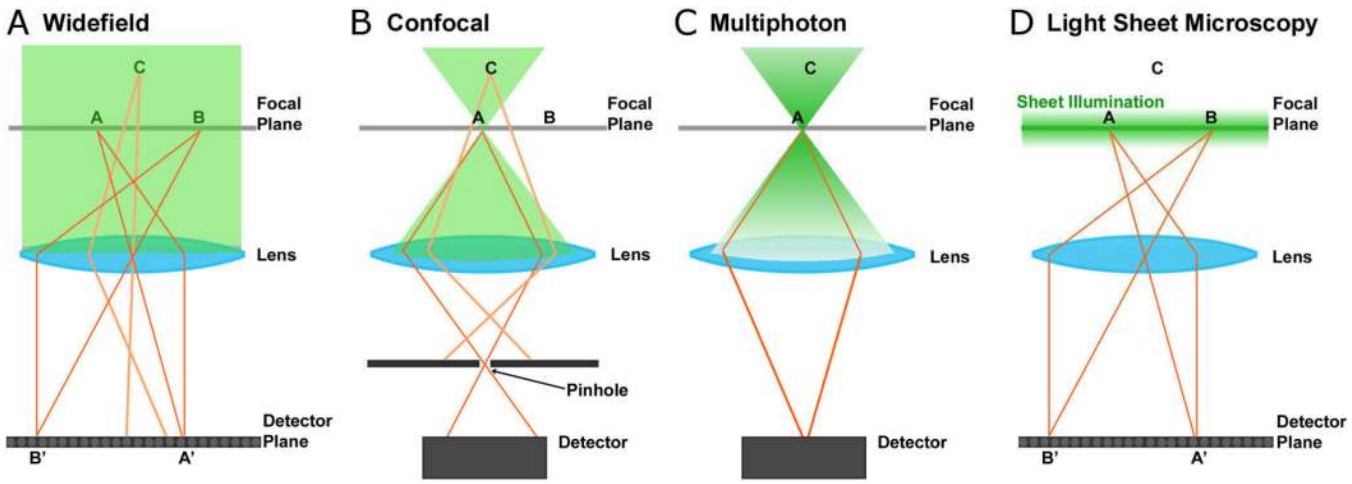

Figure 2.

Schematic illustrations of fluorescence imaging techniques: (A) wide-field, (B) point scanning confocal, (C) multi-photon, and (D) light sheet microscopy. In all diagrams, points A and B lie in the focal plane of the lens while point C lies outside the focal plane. Optical sectioning in light sheet microscopy works by creating a plane of excitation light that is coincident with the focal plane of an imaging objective. Since the sectioning occurs during excitation, the emitted light from the whole field of view can be gathered as a two-dimensional image with a standard camera.

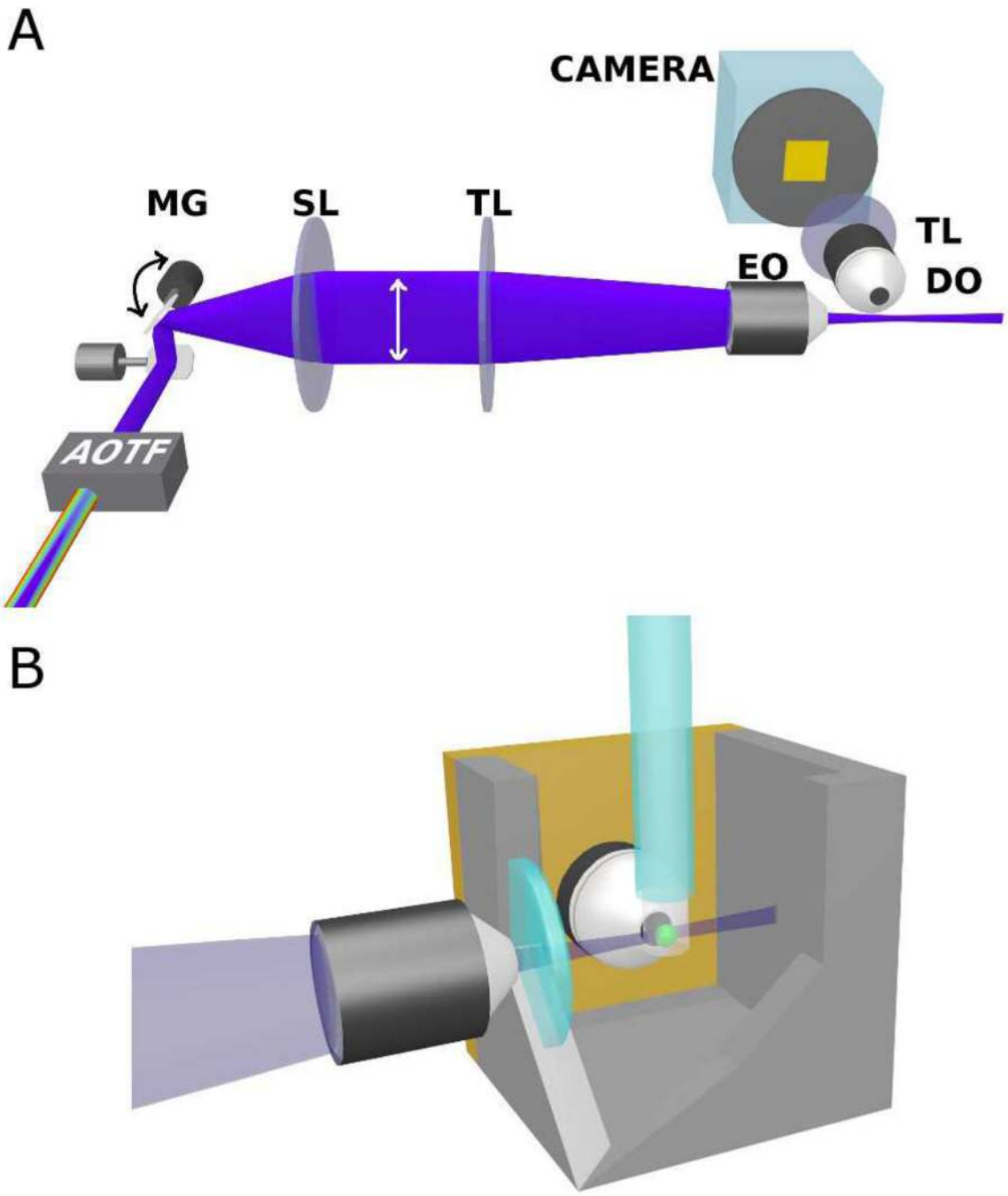

Figure 3.
(A) Schematic illustration of our light sheet microscope setup. Abbreviations: AOTF, acousto-optic tunable filter; MG, mirror galvanometer; SL, scan lens; TL, tube lens; EO, excitation objective lens; DO, detection objective lens. (B) Schematic illustration of our specimen holder, in which the EO axis, DO axis, and capillary tube are all mutually perpendicular. The green sphere denotes the specimen, which is embedded in agarose gel and held by a glass capillary from above.

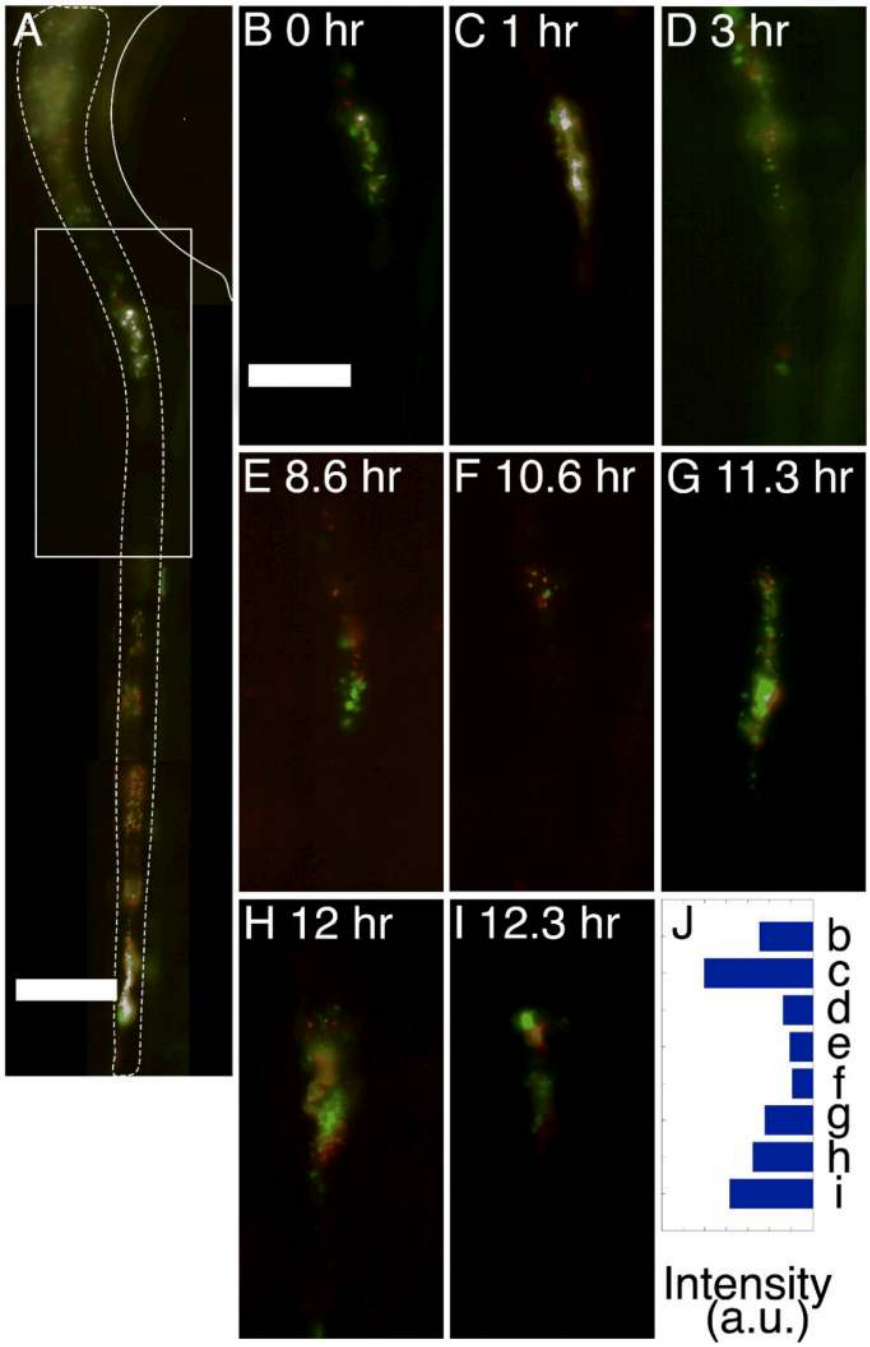

Figure 4.

Colonization of a larval zebrafish gut by GFP-expressing and dTomato-expressing *Aeromonas veronii* bacteria. (A) wild type GFP-expressing and dTomato-expressing *A. veronii* coinoculated in culture. Panels B–J show representative 2D optical sections from 3D data sets. (B) The entire gut six hours after inoculation. The gut is approximately outlined with a dashed line and the swim bladder (sb) is outlined with a solid line. (C–J) The distribution of the two microbial populations in the region corresponding to the box in (B) at various times after inoculation, with t = 6 corresponding to panel B. The contrast of each panel was independently adjusted so that the bacterial populations are clearly visible despite fluctuations in overall bacterial abundance. In each panel, both red and green intensities

were rescaled by the same amount. (J) The intensity rescaling factor in each of panels (B–I), i.e. the sum of the red and green intensities each normalized by the typical brightness of a typical bacterium, providing a measure of the total bacterial abundance at each time. Scale bars: (A) 10 microns (B–J) 100 microns

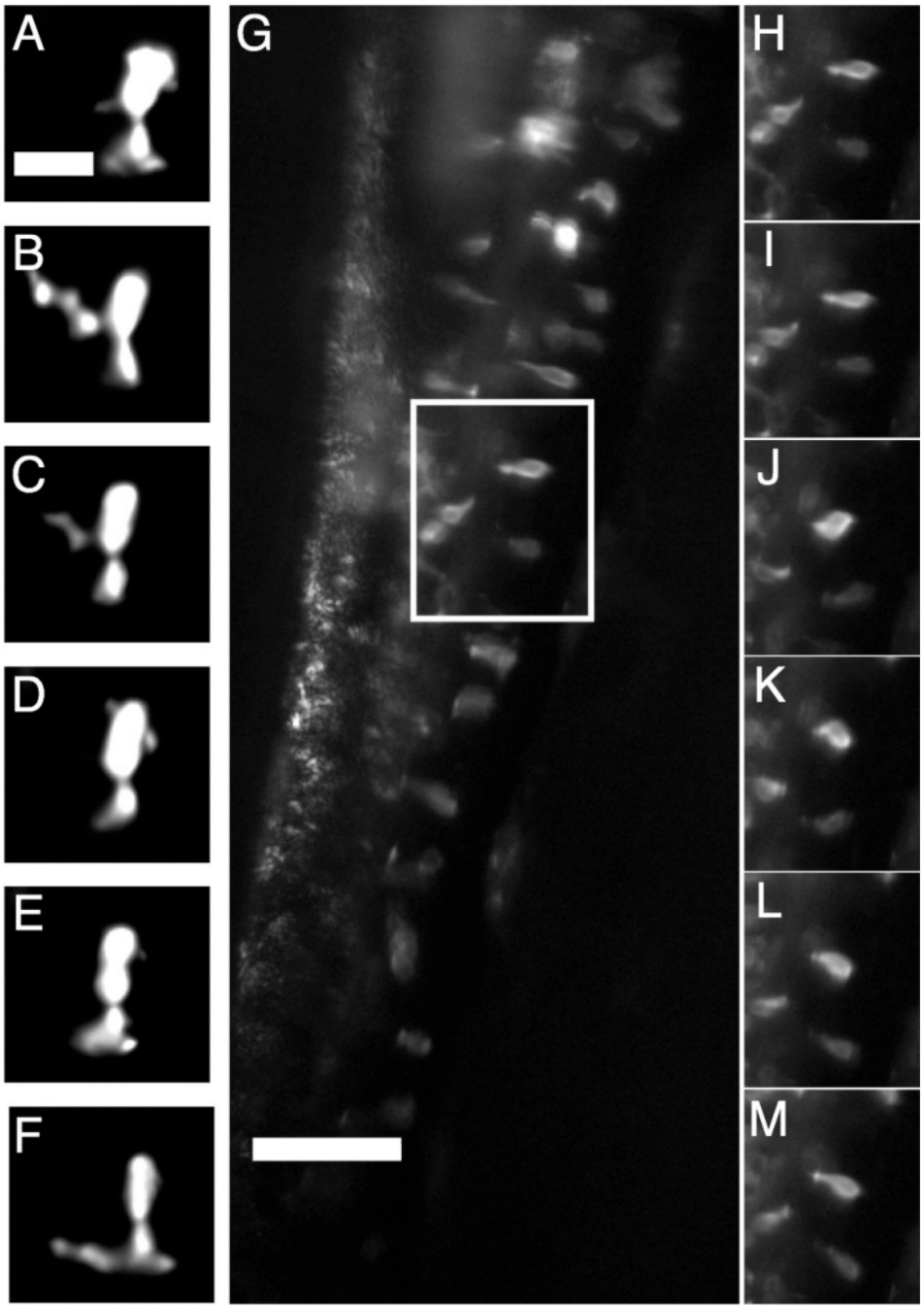

Figure 5.

(A) Fluorescently labeled enteroendocrine cells (transgenic line *nkx2.2a:egfp*) in a larval zebrafish gut. Scale bar: 40 microns. (B–G) A time series of the cells within the box in (A). The interval between each panel in (B–G) is 2.8 seconds. The deformation and movement of cells as the gut undergoes peristalsis during the imaging period is evident. The movie from which these images were taken is provided as Supplemental Movie S2. (H–M) A single fluorescently labeled neutrophil (*mpo:gfp*) within the intestinal tissue of a larval zebrafish. Each panel is a two-dimensional optical section from a three-dimensional data set, each separated in time by 2 minutes. Dynamic rearrangments of the neutrophil's filopodia are evident. Scale bar: 10 microns.

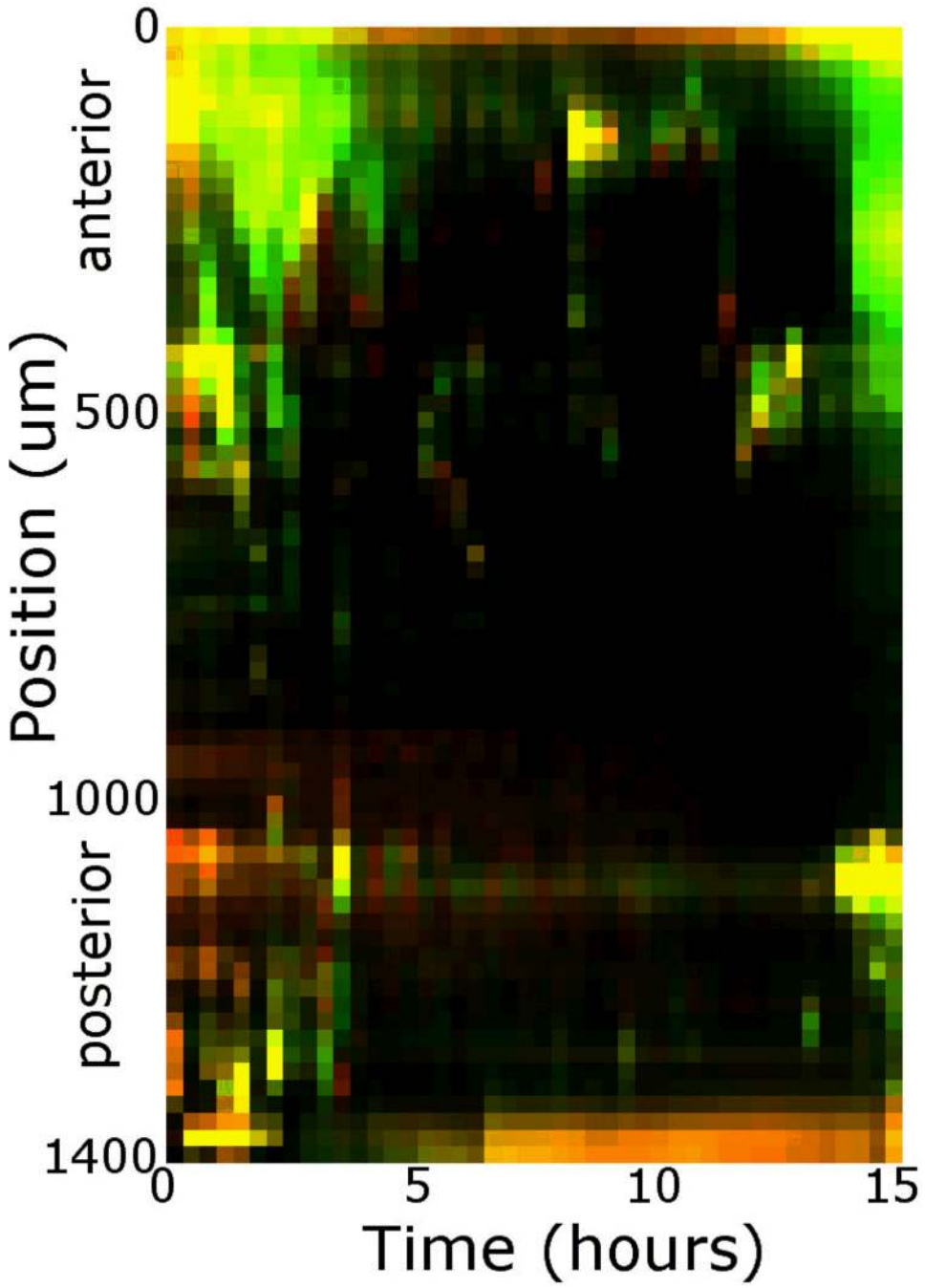

Figure 6.
Population distributions as a function of time for the two co-inoculated bacterial populations illustrated in Figure 4. Each column indicates fluorescence intensity integrated over the dimensions perpendicular to the gut axis, providing a one-dimensional measure of bacterial density along the gut, the temporal dynamics of which can be visualized in a two-dimensional plot.

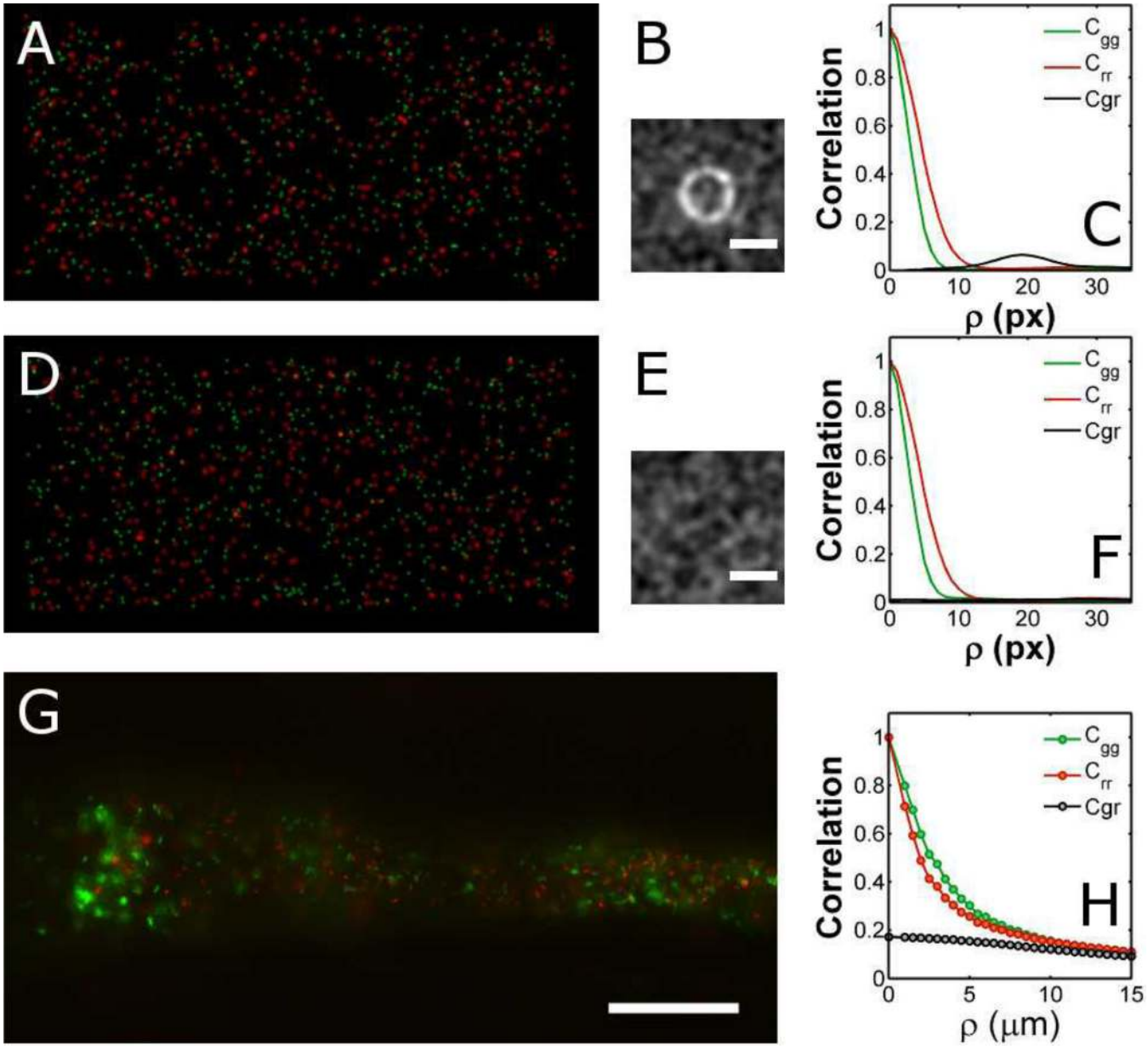

Figure 7.

Image auto- and cross-correlations. (A) A simulated two-dimensional image with randomly positioned green spots and 1.5× larger red spots each placed approximately 20 pixels from a green spot, randomly oriented. (B) The two-dimensional cross-correlation, C_{gr}, of the green and red channels of (A); a ring at a radius of 20 pixels reveals the constructed correlation. (C) The radial dependence of the auto- and cross-correlation functions; as in (B), C_{gr} shows a peak at a spatial offset of 20 pixels. (D) A simulated two-dimensional image in which both the green and red spots are positioned randomly. (E, F) the correlation functions corresponding to the image in (D). (G) A single optical slice from a three-dimensional data set depicting *Aeromonas veronii* bacteria in a larval zebrafish, as in Figure 4, at a single time point. Scale bar: 50 microns. (H) Auto- and cross-correlations of the bacterial intensity distributions calculated from the three-dimensional data set.

Table 1

List of key parts for the authors' light sheet microscope

Description	Manufacturer	Part No.
Laser 1: 488/568/647nm	Melles Griot	35-LTL-835-208
Laser 2: 594nm	Research Electro-Optics	LHYP-0201
Scan Lens	Sill Optics	S4LFT0061/065
Excitation Objective: 4× 0.10NA	Olympus Corporation	PLN 4×
Detection Objective: 40× 1.0NA	Carl Zeiss, Inc.	441452-9900-000
Mirror Galvonometer	Cambridge Technology	6210H
Stage: x, y, z Translation	Applied Scientific Instrumentation	LS-50 (×3)
Filter Wheel	Applied Scientific Instrumentation	FW-1000
Camera: 5.5 Mpx sCMOS	Cooke Corporation	pco.Edge
Deconvolution Software	Scientific Volume Imaging	Huygens Professional